IEEE Access
Multidisciplinary | Rapid Review | Open Access Journal

Received September 5, 2019, accepted September 16, 2019, date of publication October 9, 2019,
date of current version November 11, 2019.

Digital Object Identifier 10.1109/ACCESS.2019.2946521

An Improved IPM for Life Estimation of XLPE Under DC Stress Accounting for Space-Charge Effects

ZHIPENG MA, LIJUN YANG, HAORAN BIAN, MUHAMMAD SHOAIB BHUTTA, AND PENGFEI XU

State Key Laboratory of Power Transmission Equipment and System Security and New Technology, Chongqing University, Chongqing 400044, China

Corresponding author: Lijun Yang (yljcqu@cqu.edu.cn)

This work was supported by the National Key Research and Development Program of China under Grant 2016YFB0900701.

ABSTRACT Inverse power model (IPM) is often used in the engineering field to estimate the electrical life of cross-linked polyethylene (XLPE) cable insulation and describe the relationship between applied voltage and insulation failure time. The voltage tolerance index n in IPM is also used as an important factor to select appropriate AC cable thickness and pre-evaluation test voltage. However, under the influence of DC electric field, space charge accumulation changes the internal field strength of XLPE. As a result, the actual electric field strength is quite different from the applied value. Hence, the existing IPM model exhibits a large error in evaluating the electrical life of DC cables. In this paper, an improved IPM is proposed. The correction parameters α and β are introduced into the cumulative loss parameter C and voltage tolerance index n of the existing IPM to quantify the effect of space charge on distorting the electric field in electrical insulation life. Correlation between applied field strength (E_a), maximum endurance field strength (E_{rm}) and insulation failure time t of several XLPE with different thicknesses is obtained from DC voltage withstand test and pulsed electro acoustic test. In addition, the validity of the improved IPM is preliminarily verified. α and β predicted by using the space charge characteristic parameter matrix [$\boldsymbol{P}$] is proposed to efficiently obtain the actual parameters. According to experimental analysis, the improved IPM with a certain thickness is predicted by using the neural network fitting method.

INDEX TERMS Cross-linked polyethylene, space charge, inverse power model, voltage tolerance index, pulsed electro acoustic.

I. INTRODUCTION

Cross-linked polyethylene (XLPE) is the most widely used insulating material in power cables. For HVAC cable, this material has abundant operation experience, and its design method has matured [1], [2]. However, the research and development of HVDC power cable lags far behind those of HVAC cable, and most of the designs refer to the calculation methods of parameters under AC working conditions. Under DC stress, the insulation characteristic of DC cable is essentially different from that of AC cable due the characteristic relationship between resistance coefficient, temperature and electric field distortion caused by space charge accumulation in XLPE insulation [3]–[5].

The associate editor coordinating the review of this manuscript and approving it for publication was Jiajie Fan.

The life model of XLPE under electric stress is an important factor for cable insulation design. The inverse power model (IPM) $t = CE^{-n}$ is often used to describe the relationship between applied electric field (E) and failure time (t) of XLPE samples under an applied electric field. The power exponent n in the model is defined as the material voltage tolerance index and is an important basis for setting the insulation thickness and pre-qualification test voltage level during AC cable design. Therefore, XLPE may exhibit distinct lifetime characteristics due to the difference of space charge accumulation characteristics even under the same applied DC electric field.

The effect of space charge on the lifetime of XLPE under DC electric field has been widely studied [6], [7]. Various physical models i.e., Bulk, field limiting space charge (FLSC) and DMM are proposed to determine the effect of space

charge accumulation on the lifetime of materials. Among them, the Bulk model constructs the correlation between space charge distortion field strength and material activation energy and calculates the insulation life of the material under electrical and thermal stresses by using the activation energy. The FLSC model introduces the threshold field strength to establish the relationship between space charge, dielectric breakdown, and insulation life [8]. The DMM model uses charge dynamics method to analyze the effect of local stress enhancement caused by charge accumulation on insulation deterioration [9]. However, this model is complex to construct. Up to eight hypotheses are proposed and more than 10 physical parameters are introduced. Compared with that in the phenomenological model IPM, each parameter in the physical model has a clear physical meaning. The physical model quantitatively describes the influence of various factors on insulation life according to material performance deterioration. However, many factors affect material deterioration, and physical models are often complex and have limited use. In addition, this model is only applicable for theoretical research but difficult to implement for engineering applications [10]–[12]. Considering the distorted effect of space charge accumulation on the internal field strength of XLPE under DC electric field, this paper proposes an electrical life model that reflects the effect of space charge on the electrical life of XLPE. The proposed model also has a simple form and is applicable to insulation life estimation.

II. EFFECT OF SPACE CHARGE ACCUMULATION ON THE BREAKDOWN STRENGTH OF XLPE INSULATION

Short-term breakdown tests were conducted for XLPE samples with different thicknesses to study the correlation between space charge characteristics and breakdown strength of XLPE. The space charge characteristics of each sample were measured by pulsed electro acoustic (PEA) method.

The raw material of XLPE, namely, the product model LS4258DCE, used for DC cable production, was supplied by BOREALIS Company (Austria). Thin circular sheets with thickness of 50–170 μm and diameter of 50 mm were prepared by hot pressing. AC and DC short-time breakdown tests were performed according to ASTM-149 standard [13]. The voltage increment rate was 1 kV/s, and more than 10 samples were tested at each point.

Two groups of samples labeled group A and B were prepared by two operators using the same preparation process to avoid the influence of sample difference on test results.

The test results in Fig. 1 indicate that with the increase in thickness d, the AC breakdown strength E_{b-ac} decreases continuously, whereas the DC breakdown strength E_{b-dc} increases first and then decreases. The E_{b-dc} of 100 μm sample is approximately 1.3 times of that of 60 μm sample. Some differences were found in the results of group A and group B, possibly due to the sample preparation of different operators. However, the variation rule of breakdown strength with thickness is consistent.

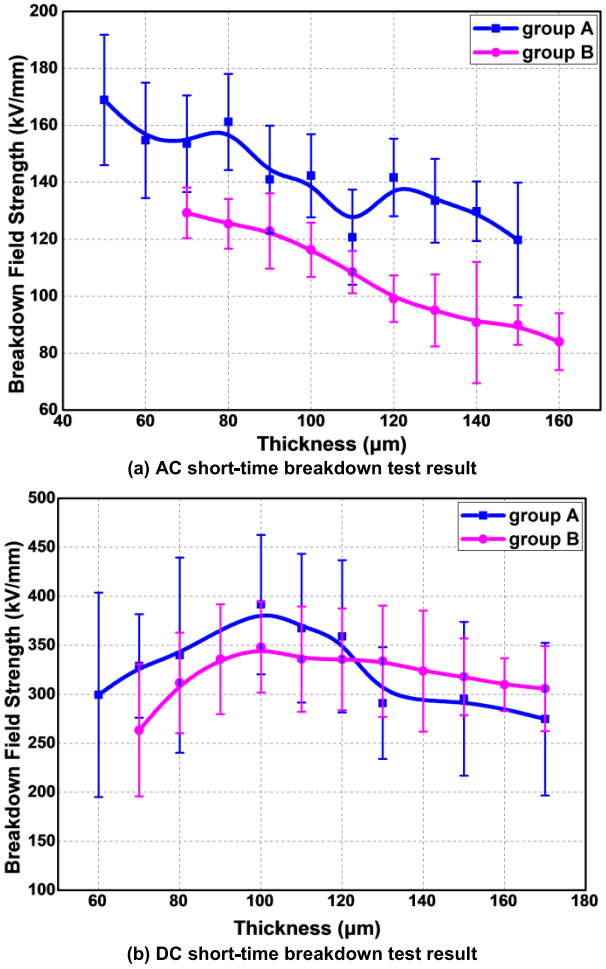

FIGURE 1. Variation of breakdown strength E_b with thickness d under (a) AC and (b) DC electric fields.

According to the "volume effect" of solid dielectrics, the breakdown strength of XLPE is strongly dependent to thickness and normally decrease with the increasing thickness. Breakdown always occurs at the weak points of the dielectric material that are caused by local defects. The increasing volume of material caused by increase in thickness or area will increase the probability of local defects occurrence but reduce the breakdown strength. This volume effect has been widely observed and recognized through the breakdown characteristics of various insulating materials, both under AC and DC [14]–[16].

In this study, the volume effect is valid for all film samples under AC. Hence, the E_{b-ac} decreases with increasing film thickness. However, the volume effect is not dominant for all thicknesses in the case of DC. The E_{b-dc} increases with the increasing thickness in the range of $d < 100$ μm but decreases in the range of $d > 100$ μm.

Similar phenomena were previously observed. Riechert *et al.* [17] investigated the DC breakdown characteristic of XLPE. Although the author claimed that insulation thickness between 50 and 200 μm did not substantially influence the short-term electrical strength of XLPE, experimental

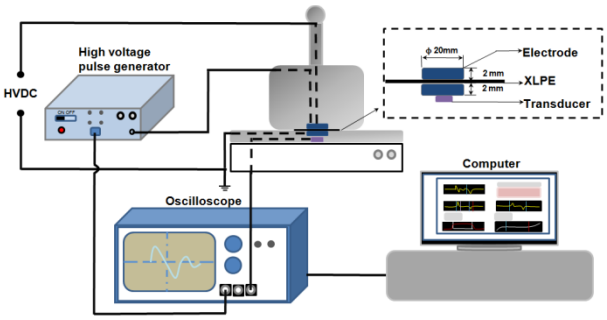

FIGURE 2. Space charge characteristic test platform.

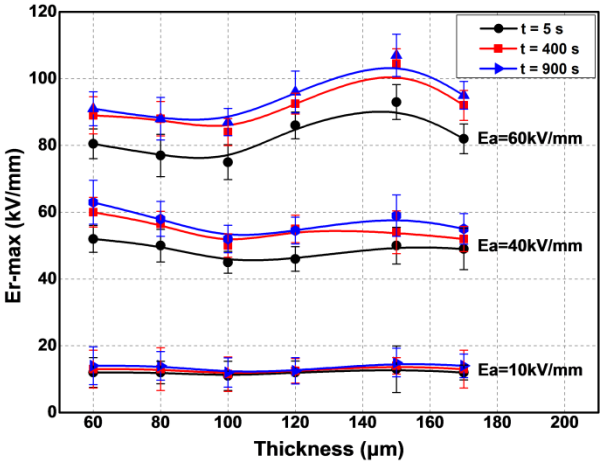

FIGURE 3. Variation of maximum field strength in samples with different thicknesses.

results proved that the E_{b-dc} increased first, then decreased, and approached its maximum value at $d = 160$ μm. This value was approximately 105% of that at $d = 100$ μm. Khazaka *et al.* [18] investigated the parylene F (PA-F) film. The DC breakdown strength increased with the increasing thicknesses from 1.4 μm to 5 μm followed by a decrease for high thicknesses. Wang [19] studied the thickness dependence of the breakdown characteristics of polyester film for AC and DC. The results indicated that E_{b-dc} increased from 402.5 kV/mm at $d = 40$ μm to 417.5 kV/mm at $d = 50$ μm and then decreased to 318.2 kV/mm at $d = 110$ μm. The E_{b-ac} continued to decline with the increase in thickness. Li *et al.* [20] studied the breakdown characteristics of oil-impregnated insulation paper (OIIP) under AC, DC and pulsating DC voltages. The results revealed that breakdown strength decreased with the increasing thickness in the thickness range of 50 μm to 200 μm under AC. However, this parameter slightly increased with the increasing thickness of OIIPs under pulsating DC voltages (ripple factor of pulsating voltages = 1, 1/3) and strongly increased under DC voltages. The breakdown strength of 130.58 kV/mm at 50 μm thickness remarkably increased to 161.76 kV/mm at 200 μm.

Most reports only provided experimental results and revealed the difference in the thickness dependence of breakdown strength under AC and DC. Only a few investigated the reason and mechanism behind this phenomenon. Some scholars ascribed the increase in E_{b-dc} to the increase of crystallinity and the absence of spherulites within the sample film [18] or to the low free volume or electron mean free path in the thin film [21]. However, these analyses were only hypothesis and conjectures and have not been fully tested.

Nevertheless, one thing is certain that, in addition to volume effect, other factors may play a dominant role in DC breakdown, especially for thin samples and high electric fields. In this study, we assume that the distortion of electrical field caused by space charge accumulation contributes to this phenomenon.

For experimental verification, the space charge characteristics of XLPE samples were measured by PEA experiment. The composition of the test circuit is shown in Fig. 2. According to JB/T 12927-2016 standard for measuring space charge distribution in solid insulating materials [22], if the x-axis denotes the thickness direction of the sheet sample, then the charge density along the thickness direction at voltage applying time t is $\rho(x, t)$. The actual electric field strength inside the sample, $E_r(x, t)$, can be determined by Poisson equation according to (1).

$$E_r(x,t) = \frac{1}{\varepsilon_0 \varepsilon_r} \int \rho(x,t) dx \tag{1}$$

where ε_0 and ε_r are the vacuum dielectric constant and relative dielectric constant of the sample respectively.

Given that insulation failure is mainly attributed to the maximum electric field inside the sample, E_{r-max} is defined as the maximum of $E_r(x, t_i)$ that is actually experienced by the sample at t_i, and Fig. 3 shows the relationship between E_{r-max} and d. The results of $t_i = 5$, 400, 900 s, and $E_a = 10$, 40, 60 kV/mm are presented to illustrate the influence of t and E_a on the relationship between E_{r-max} and d. When d increases, E_{r-max} decreases first and then increases. This tendency is observed at each value of t and E_a.

The space charge distorts the field strength inside the sample, making the actual value stronger than the applied one. The degree of distortion increases with the applied field strength. In the range of $d = 50 - 100$ μm, the E_{r-max} decreases with the increase in d. This finding indicates that the distortion of the field strength caused by space charge accumulation is weakened within this thickness range. This phenomenon occurs mainly because the injection of homogeneous space charge weakens the applied electric field strength and thus suppressesthe injection of space charge. Moreover, the short-term breakdown strength of XLPE increases with the thickness. E_{r-max} increases slightly with d in the range of $d > 100$ μm. This result indicates that the effect of space charge accumulation on the field strength distortion is enhanced in this thickness range. This phenomenon mainly occurs because the increase in the thickness of the XLPE enhances the number of traps in bulk due to increase in amorphous regions in thicker samples, which leads to enhancement of the space charge accumulation and the increase

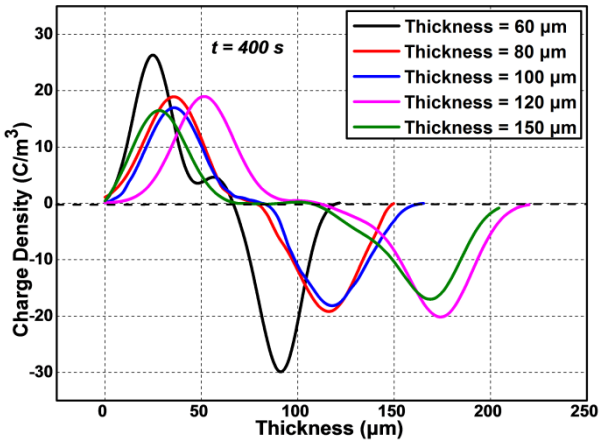

FIGURE 4. Charge density distribution with various thicknesses.

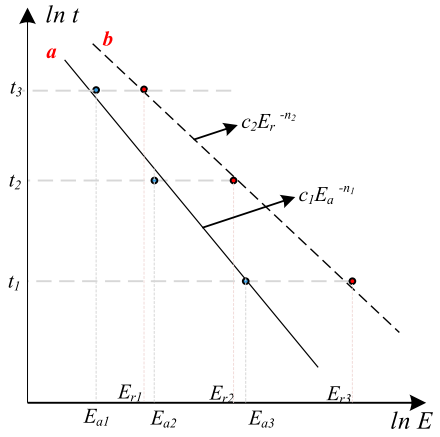

FIGURE 5. IPM life curve with regard to space charge distortion effect.

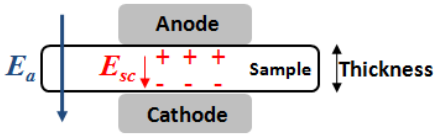

FIGURE 6. Internal electric field formed by space charge accumulation.

of E_{r-max}. As a result, the breakdown strength of XLPE decreases with d in range of $d > 100$ μm.

E_{r-max} is affected by space charge accumulation at various thicknesses. This phenomenon can also be explained by the space charge distribution curve. Fig. 4 shows the charge density distribution of the samples with different thicknesses of 60, 80, 100, 120, and 150 μm. The distribution curve for every sample was measured under an applied electric field of 40 kV/mm at 400 s.

It can be seen from Fig. 4, in the range of $d = 50-100$ μm, the space charge accumulation of 60 μm XLPE near the two electrodes is stronger than that of 80 and 100 μm XLPE. This finding indicates the decreasing trend of $E_r(x, t)$ in this thickness range. Similarly, E_{r-max} should have the same decrease trend. The minimum amount of charge accumulation near the electrode of the 100 μm XLPE corresponds to the minimum E_{r-max}, which is consistent with the result in Fig. 3. In the range of $d > 100$ μm and near the two electrodes, 120 μm XLPE accumulates more charge than 100 and 150 μm XLPE. As shown in Fig. 3, the E_{r-max} of 120 μm XLPE is higher than that of 100 and 150 μm XLPE. In summary, E_{r-max} increases slightly with thickness in the range of $d > 100$ μm.

The variation in thickness shows the relationship between space charge accumulation and DC breakdown strength. The electric field distortion caused by space charge accumulation is closely related to the DC breakdown strength of XLPE.

III. IMPROVED IPM ELECTRICAL LIFE MODEL WITH REGARD TO SPACE CHARGE EFFECTS

A. PROPOSED IMPROVED IPM

The inverse power model shown in (2) is often used as the electrical life model of XLPE.

$$t = CE^{-n} \tag{2}$$

where E is the electric field strength in kV/mm, t is the failure time or life in s. C is a constant representing the cumulative electrical damage required for material failure, and n is the voltage tolerance index representing the degree of influence of electric field change on insulation life. The failure times t_1, t_2, and t_3 were recorded under at least three different applied field strengths E_{a1}, E_{a2}, and E_{a3}. A line was drawn on the logarithmic coordinates of *lnt-lnE*, and the values of n and C were fitted as shown in line a in Fig. 5.

With regard to the field distortion effect caused by space charge, the actual field strength E_r is not equal to the applied field strength E_a but is determined by E_a and the field strength E_{sc} formed by the space charge inside the insulation. This finding satisfies (3) as shown in Fig. 6.

$$E_r = E_a + E_{sc} \tag{3}$$

Actually, the IPM of the samples should be a straight line b as shown in the Fig. 5. Space charge distorts the actual field strength (E_r) inside the sample. Moreover, line a (E_a-$t$curve) shifts and rotates on the basis of line b (E_r-$t$curve). Correction parameters α and β can be added into the IPM of (2) as shown in (4) to describe the correlation between the two curves.

$$\mathrm{t} = C_r^{\alpha} E_r^{-\beta n_r} \tag{4}$$

which can be expressed as:

$$\ln t = \alpha \ln C_r - \beta n_r \ln E_r \tag{5}$$

where α, β are defined as shifting and rotation factor, respectively; and E_a-t curve represents double logarithmic coordinate system that can be obtained by multiplying the intercept and slope of E_r-t curve by α, β that is equivalent to the shift and rotation of E_r-t curve up and down, respectively. The difference between E_r and E_a is mainly caused by the field distortion due to the space charge accumulation. Hence, the values of α and β are closely related to the space charge characteristics of the sample.

B. ACQUISITION OF IMPROVED IPM MODEL PARAMETERS

1) ACQUISITION OF $E_a - t$ AND $E_{rm} - t$ CURVES

To obtain the parameters of the improved IPM proposed above, we proposed the following hypotheses:

- Under a uniform applied electric field (E_a), the failure of XLPE sample depends mainly on the maximum of E_r inside the XLPE, namely, E_{r-max}.
- The relationship between E_r and failure time t satisfies the inverse power function shown in (6). At an evaluated temperature, the voltage tolerance index (n_r) and cumulative loss parameter (C_r) in the formula are constant and are only related to the physical and chemical properties of XLPE itself. Both constants have no relationship with the size of the sample. E_r-t curve is defined as the intrinsic life curve (ILC) of XLPE.

$$t = C_r E_r^{-n_r} \tag{6}$$

- The difference in E_a leads to the variation of space charge accumulation and field strength distortion at various degrees. The value of actual field strength $E_r(x, t)$ inside XLPE is determined by E_a and the distribution characteristics of space charge e.g., $\rho(x, t)$.

The above hypothesis states that although thickness does not affect the E_r-t curve of XLPE, it will change the space charge density $\rho(x, t)$ in XLPE. Under the same applied field strength (E_a), the actual field strength (E_r) in the sample is quite different. Hence, the breakdown strength E_a and corresponding E_a-t curves at different thickness are also varying. Therefore, this hypothesis does not contradict the volume effect of solid dielectrics. Here we can define E_a-t curve as the apparent life curve (ALC) of XLPE.

XLPE samples with thicknesses of 60, 70, and 80 μm were prepared for voltage withstanding tests at E_a of 180, 200, and 220 kV/mm to verify the above hypothesis. The setup in Fig. 2 was used to simultaneously launch voltage withstand and space charge tests. Space charge density $\rho(x, t)$ was recorded at intervals of 60 s until sample breakdown. The corresponding $E_r(x, t)$ was calculated according to (1). Fig.7 shows the variation of $E_{\mathrm{r}}(x)$ along the thickness direction at different voltage applying time. For brevity, only the result of 60μm sample at E_a of 180kV/mm was presented. $E_{\mathrm{r-max}}$ appears in the middle of the sample and is greater than the applied field strength E_a. $E_{\mathrm{r-max}}$ increases gradually over the first 420 s and then becomes relatively stable. In this case, the stable $E_{\mathrm{r-max}}$ in sample is 17% greater than that applied strength, $E_a = 180$ kV/mm.

Fig. 8 shows the variation of E_{r-max} with endurance time of DC field, where t_b is the corresponding failure time in s. For brevity, only the result of 60 μm sample was presented. E_{r-max} first increases with endurance time, then reaches a stable value, and fluctuates slightly up or down the value. Owing to E_{r-max} fluctuation over time, its root -mean -square (RMS) was used to calculate the relationship between E_r and

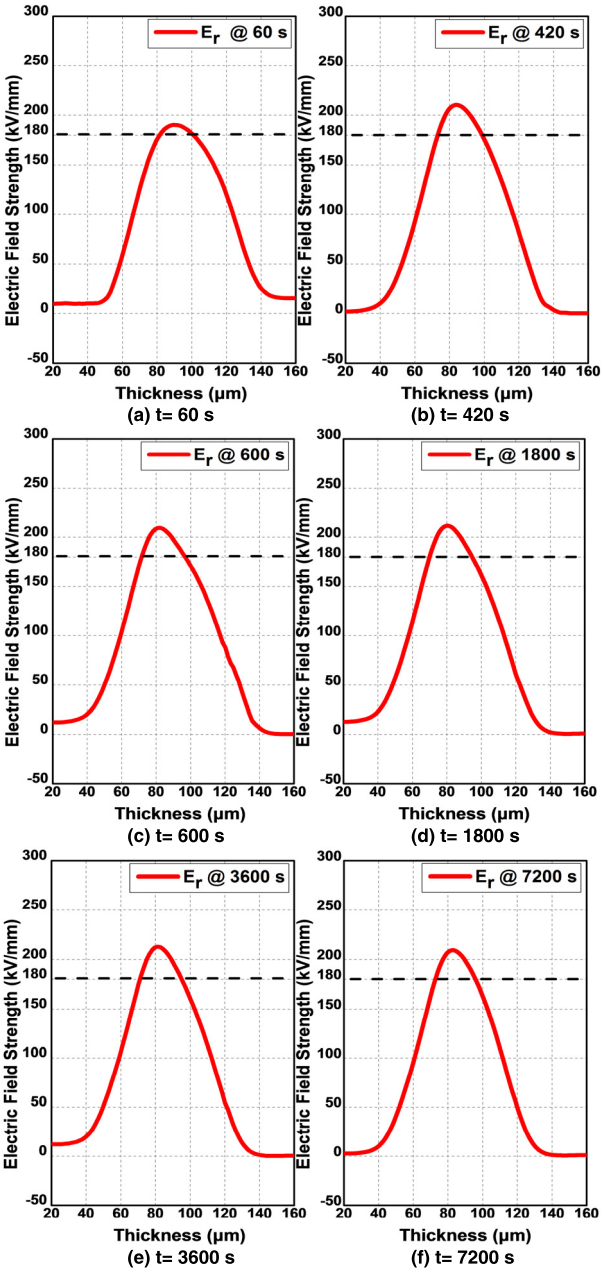

FIGURE 7. Distribution of E_r along the thickness direction at different voltage applying time.

failure time as shown in (7).

$$E_{rm} = \sqrt{\sum_{i=1}^{N} E_{r-\max}^2(t_i)/N} \tag{7}$$

where t_i is the sampling point (at intervals of 60 s) and N is the total sampling times during the whole endurance test, until breakdown.

Considering the statistical characteristics of XLPE failure time, four to five life tests were conducted under each value of applied field strength E_a, where t_b is in s and E_{rm} is in kV/mm. The results are shown in Table 1.

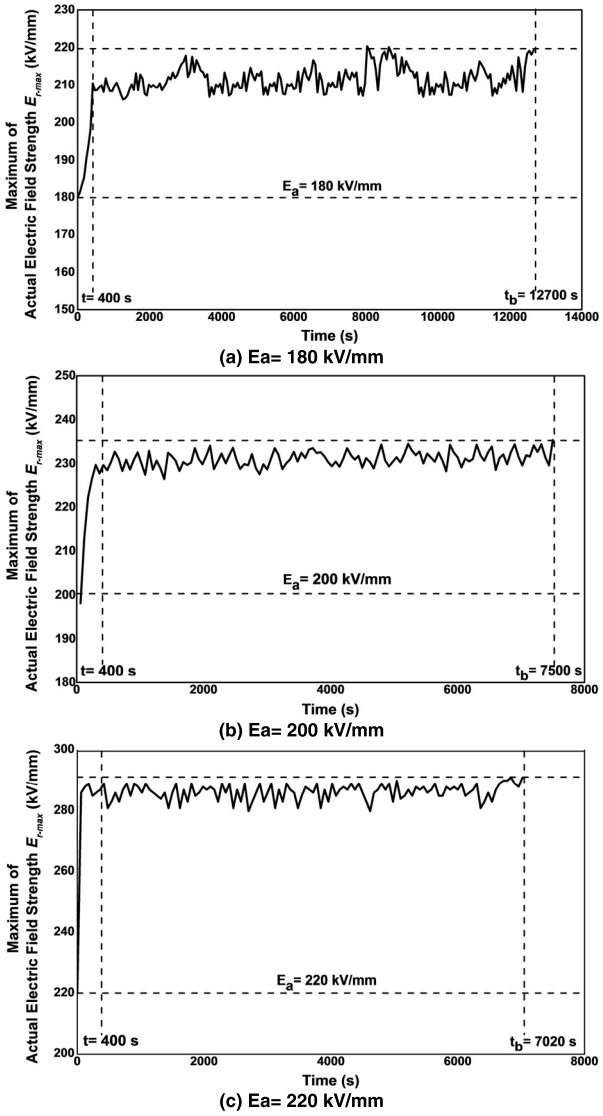

FIGURE 8. Variation of E_{r-max} with endurance time of DC.

TABLE 1. Parameter t_b and E_{rm} under different E_a values.

E_a	180 kV/mm		200 kV/mm		220 kV/mm	
	t_b	E_{rm}	t_b	E_{rm}	t_b	E_{rm}
	14585	216.2	5740	249.9	1920	280.3
	12700	210.8	6960	239.9	2565	285.5
	16960	221.9	7500	245.1	4380	299.3
	18450	209.8	9480	235.7	7020	288.6
	—	—	10100	240.6	—	—

The data in Table 1 obey the two-parameter Weibull distribution model which is used to analyze the parameters t_b and E_{rm}. Furthermore, the parameters with a failure probability of 63.2% were obtained and are shown in Table 2.

Weibull statistical data in Table 2 can be plotted in a double logarithmic coordinate system as the ordinate and abscissa in the life curve (*lnt-lnE*) as shown in Fig. 9.

TABLE 2. Weibull statistics of parameters t_b and E_{rm}.

E_a	Weibull statistics	
180 kV/mm	t_b	16788
	E_{rm}	217.5
200 kV/mm	t_b	9461.2
	E_{rm}	244.9
220 kV/mm	t_b	5280
	E_{rm}	292.4

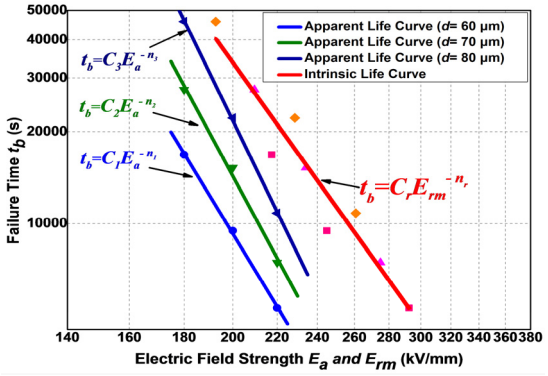

FIGURE 9. Life curves of samples with different thicknesses.

Fig. 9 shows that among the samples with three different thicknesses, the ALC, which is the E_a-t curves, satisfies the IPM. The parameters of the model vary with the thickness of the samples. The parameters n and C increase with the thickness of the samples. However, the E_{rm}-t data corresponding to the three thickness samples can be fitted by one straight line (namely ILC) in the double logarithmic coordinate system. This finding indicates that the change of thickness does not affect the parameters of IPM obtained from ILC. In addition, experimental results validate the hypothesis that the relationship between E_r and failure time satisfies the inverse power function as shown in (6). At a certain temperature, the n_r and C_r in this equation are constant, are only related to the physical and chemical properties of the sample itself and are independent of the sample size.

2) CALCULATIONS OF CORRECTION PARAMETERS α AND β

Table 3 gives the improved IPM parameters. $n_1 - n_3$ AND C_1–C_3, for three different thickness samples were determined by ALC. n_r, and C_r were determined by ILC.

According to the improved IPM proposed in (4), the parameters of shifting factor (α) and rotation factor (β) can be calculated based on the correlation of n_i, C_i, and n_r, C_r, which are listed in Table 3. For the 60 μm sample, its ALC parameter, C_1, can be obtained by taking exponent 1.092 from the ILC parameter, $C_r = 5.92 \times 10^{15}$, and n_1 can be obtained by multiplying $n_r = 4.89$ with 1.178. This value is equivalent to rotating the ILC at a certain angle and

TABLE 3. Improved IPM parameters.

d(μm)	n		C		α	β
-	n_r	4.89	C_r	5.92×10^{15}	1	1
60	n_1	5.76	C_1	1.65×10^{17}	1.092	1.178
70	n_2	6.49	C_2	1.22×10^{19}	1.210	1.327
80	n_3	7.20	C_3	8.20×10^{20}	1.326	1.472

translating it downward for a certain distance in logarithmic coordinates.

IV. A METHOD OF OBTAINING IMPROVED IPM PARAMETERS BASED ON SPACE CHARGE CHARACTERISTICS

According to the above analysis, the ALC of a sample with different thicknesses can be obtained when the parameters of ILC are known. This method can also be used to describe the failure time of the sample under different applied field strengths.

In Section III, the parameters of the improved IPM, α, β, C_r and n_r, were obtained. For practical application, the above methods have a heavy workload. For the improved IPM, its parameters are mainly caused by the difference between the applied field strength (E_a) and the actual field strength (E_{r-max}) due to space charge accumulation. Therefore, the space charge characteristics parameters are considered as closely related to α, β, C_r and n_r. If the parameter $\boldsymbol{P}$ describing the space charge characteristics of the XLPE is used to quantitatively calculate α, β, C_r and n_r, then the ALC of the sample can be obtained conveniently and efficiently.

A. SELECTION OF SPACE CHARGE CHARACTERISTIC PARAMETER MATRIX [P]

Many parameters, including time- and field-varying ones, describe the characteristics of space charge. Montanari and Fabiani [23], [24] used space charge measurements and accelerated life tests to evaluate the performance of cable insulation under DC stress. By referring to the space charge parameters proposed by G. C. Montanari, this paper adopts the matrix $[\boldsymbol{P}] = [\mathrm{P_1}, \mathrm{P_2}, \ldots \mathrm{P_k}]$ to represents the space charge behavior of XLPE. Each parameter is defined as follows:

- Maximum field strength distortion rate (k_{max})

The ratio of maximum field strength E_{r-max} to applied field strength (E_a) is defined as field strength distortion rate $k = E_{r-max}/E_a$. The maximum value of k in a certain pressure period is counted as parameter k_{max}.

- Mean field strength distortion rate (k_{mean})

Similarly, the average value of k in a certain pressure period is counted as the parameter k_{mean}.

- Average bulk density of space charge (Q)

If the charge density at time t_i is $\rho(x, t)$, then the average bulk density of the space charge can be calculated by (8) [22].

$$Q = (\sum_{i=1}^{N} \frac{1}{x_1 - x_0} \int_{x_0}^{x_1} |\rho\,(x, t_i)|dx)/N \tag{8}$$

where x_0 and x_1 are the positions of the electrodes, t_i represents the i test times within a certain pressure period, and N represents the total test times of space charge characteristics during the pressure period.

- Space charge accumulation rate (b)

When different E_a values are applied to the sample, the average bulk density Q increases with E_a. According to space charge limiting current theory, Q has different increasing rates corresponding to different applied field strength ranges. Q increases linearly with E_a in the space charge limited current region. The rate of space charge accumulation can be expressed by the slope b of Q growth curve [25].

Sample thickness d and applied field strength E_a can also be included in the parameter matrix $[\boldsymbol{P}]$ as two auxiliary parameters.

In conclusion, the parameters of space charge characteristics can be expressed by parameter matrix as follows:

$$[P] = [d, E_a, k_{\max}, k_{mean}, \mathrm{Q}, b] \tag{9}$$

According to Figs. 7 and 8, E_{r-max} takes approximately 400 s to stabilize after pressure. Therefore, in this part of PEA test, the sampling interval was set to 5 s, and the sample was continuously pressurized for 900 s. The test data between 400 s and 900 s were used to calculate the parameters k_{max}, k_{mean}, Q and b. For the XLPE with three thicknesses of 60, 70, and 80 μm, the data were extracted from Part III section B. PEA tests were conducted under five different applied field strengths of 80, 100, 120, 140, and 160 kV/mm, and space charge characteristic parameters were extracted to form matrix $[\boldsymbol{P}]$. The results are shown in Table 4.

B. ESTABLISHMENT OF THE RELATIONSHIP BETWEEN [P] AND α & β

In this part, the correction parameters α and β of IPM were predicted by matrix $[\boldsymbol{P}]$. When this function is realized, only the space charge characteristics of the sample can be tested, and the lifetime model parameters n and C can be calculated or predicted without tedious and time-consuming electrical lifetime tests. In this study, BP neural network fitting method was used to calculate the IPM correction parameters of samples with the space charge parameter matrix $[\boldsymbol{P}]$ as the input and $[\boldsymbol{\alpha}, \boldsymbol{\beta}]$ as the output. A multi-layer feedforward neural network, which is based on error back propagation algorithm and has strong non-linear mapping ability, was selected. The number of nodes in the input, output and hidden layer are 6, 2, and 15, respectively. Fig. 10 shows the structure of the neural network.

First, we used teaching samples to train the network parameters. In the teaching samples, the parameters of

TABLE 4. Parameter matrix.

No.#	d (μm)	E_a (kV/mm)	k_{max}	k_{mean}	Q (C/m^3)	b
1	60	80	1.453	1.431	56.95	
2	60	100	1.540	1.511	74.09	
3	60	120	1.883	1.770	113.00	1.307
4	60	140	1.623	1.594	124.26	
5	60	160	1.690	1.664	133.16	
6	70	80	1.288	1.248	45.15	
7	70	100	1.506	1.463	67.06	
8	70	120	1.604	1.565	86.46	1.392
9	70	140	1.480	1.468	100.30	
10	70	160	1.345	1.332	121.19	
11	80	80	1.293	1.259	50.38	
12	80	100	1.262	1.224	57.59	
13	80	120	1.306	1.283	70.76	1.135
14	80	140	1.305	1.284	91.37	
15	80	160	1.248	1.230	108.06	

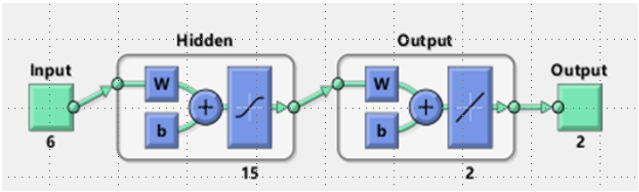

FIGURE 10. Structure of the neural network.

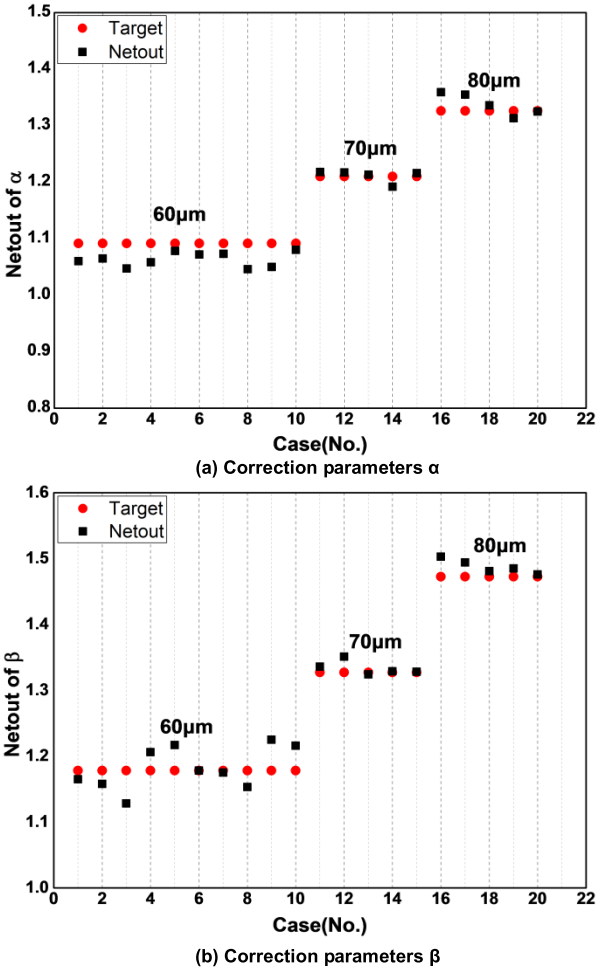

FIGURE 11. Prediction results of neural network for the correction parameters of test samples.

Train1–Train15 of 15 samples shown in Table 4 are selected as input $[\boldsymbol{P}]_{train}$, and the correction coefficient matrix corresponding to each sample in Table 3 are used as output $[\boldsymbol{\alpha}, \boldsymbol{\beta}]_{train}$. Levenberg-Marquardt algorithm was used to train the hidden layer neurons, and mean square error was used to evaluate the effect of network training.

Another 20 samples of case 1–case 20 were selected as the test objects to verify the predictive effect of the network after training. The thickness of case 1–case 10 samples is 60 μm, that of case 11–case 15 is 70 μm, and the remaining samples' thickness is 80 μm. The space charge parameter matrix $[\boldsymbol{P}]_{test}$ of these 20 samples was used as the input of the network, and the IPM correction parameter of the test samples was applied as the output of the network $[\boldsymbol{\alpha}, \boldsymbol{\beta}]_{test}$. This parameter, was also used to determine its electrical life model parameters.

Fig. 11 shows the comparison between the network prediction value "Netout" and the target value "Target". For the test samples of 60, 70, and 80 μm, the prediction errors of parameters α and β by the neural network are small (standard deviation$<$ 5%), which preliminarily proves the validity of the method.

V. DISCUSSION

Although the above research preliminarily confirms the effectiveness of the improved IPM proposed in this paper, the neural network obtained in part B of section IV can only accurately predict the IPM model correction parameters of samples with thickness of 60–80 μm due to the limited number of teaching samples participating in the training.

ALC and its corresponding space charge characteristic matrix $[\boldsymbol{P}]$ of additional samples with wide thickness range must be tested and trained to produce an abundant teaching sample and to improve the prediction ability of the neural network and predict the α and β of thick samples. Admittedly, this process require a long testing time, especially through the use of constant DC withstand voltage method to obtain electrical life data.

The PEA test was used for the voltage withstand test on the thin sample to confirm the relationship between the distortion field caused by space charge and the apparent lifetime curve E_a-t of XLPE. This examination aims to obtain the E_a-t curve and the real field strength inside the dielectric material by measuring the space charge characteristics to consequently obtain the intrinsic life curve E_r-t. However, apply this method is not feasible to predict the life model parameters of thick samples and real cable insulation. The DC power supply of PEA space charge test platform is not

designed for high voltage withstand test, and the maximum DC voltage output of this platform usually does not exceed 20 kV. The electrical life test is difficult to actualize with sample breakdown as the end of life for thick samples. Moreover, the frequent breakdown of test samples on PEA test platform will greatly damage the performance of the platform. This reason also explains why teaching sample data with thickness greater than 80 μm were not obtained in this paper.

Given the importance of E_r-t curve for the determination of α and β, this parameter requires simultaneous voltage withstand and space charge characteristic tests, which cannot be well achieved by current testing methods. So, how to apply this method to the lifetime model of real cables? As shown in Fig. 9, since E_r-t can be obtained from the apparent lifetime curve E_a-t of the sample with different thickness (d_1, d_2, d_3 $\ldots\ldots d_n$) by combining the shifting factor [α_1, α_2, $\alpha_3 \ldots \alpha_n$] and the rotation factor [β_1, β_2, $\beta_3 \ldots \beta_n$], then the E_r-t of any thickness sample can also be obtained from the E_a-t of other thickness samples by appropriate α and β transformations. This finding indicates that instead of necessarily obtaining the E_r-t lifetime curve of the material, we can select a sample with a specific thickness (e.g. 0.5 mm or 1.0 mm) as the reference sample and measure its apparent life curve E_a^{ref}-t to replace the E_r-t mentioned above. Subsequently, we can test the life curve E_a^i-t of other samples with thickness d_i and calculate the rotation and shifting factor between the E_a^i-t and E_a^{ref}-t curves of the reference sample. We can also examine the space charge parameter matrix of these samples and obtain enough teaching samples based on the method in section IV to train the neural network. When the neural network has reliable prediction ability, we can only test the matrix [$\boldsymbol{P}$] of the insulation of an unknown cable in practice and use it as the input of the neural network to predict the IPM electrical life model of the real cable. The predictive ability and accuracy of the neural network also depend on the abundance and sufficiency of the teaching samples. In addition, obtaining $E_a - t$ and then the teaching samples by constant DC withstand voltage method is still time consuming and arduous. Fortunately, step stress test can be used to improve the efficiency of life test by setting reasonable test parameters [26]. We can easily obtain the $E_a - t$ curve of the real cable insulation as long as the DC power supply meets the test requirements. For the measurement of space charge characteristics, full-scale real cable testing devices are already available [27], [28]. Therefore, the proposed method theoretically has the prospects of engineering application in real cables. That is also the research content we are carrying out.

VI. CONCLUSION

An improved IPM electrical life model is proposed based on the distortion effect of space charge accumulation on the internal field strength of XLPE insulation to quantify the effect of space charge accumulation on the electrical life characteristics of XLPE samples under DC electric field. In the existing IPM model, the correction coefficients α and β are introduced to quantify the effect of space charge distortion field on insulation electrical life. The relationship between the intrinsic lifetime curve $E_r - t$ and the apparent lifetime curve $E_a - t$ of XLPE samples with different thickness are studied by DC withstand lifetime and space charge characteristic tests, and the rationality of the proposed model is preliminarily verified. Furthermore, correlation calculation and prediction method for correction coefficients α and β are proposed by using the space charge parameter matrix. The validity of this method is preliminarily validated by using a thin sample ($d = 60 - 80$ μm), and the possible application of this method to real cables is discussed.

REFERENCES

[1] *Recommendations for Testing DC Extruded Cable Systems for Power Transmission at a Rated Voltage Up to 500 kV*, CIGRE, Paris, France, 2012.
[2] B. H. Ouyang, S. H. Liu, and X. B. Deng, "Optimization design for insulation thickness of high-voltage XLPE cable," *High Voltage Eng.*, vol. 42, no. 8, pp. 2388–2393, Aug. 2016.
[3] H. Ghorbani, A. Abbasi, M. Jeroense, A. Gustafsson, and M. Saltzer, "Electrical characterization of extruded DC cable insulation—The challenge of scaling," *IEEE Trans. Dielectr. Electr. Insul.*, vol. 24, no. 3, pp. 1465–1475, Jun. 2017.
[4] M. Hu, S. H. Xie, J. Xue, and J. Zhang, "Design and test of China first ±160 kV DC cable for flexible DC transmission project," in *Proc. China Int. Conf. Electr. Distrib. (CICED)*, Sep. 2014, pp. 1680–1684.
[5] H. Ghorbani, M. Jeroense, M. Saltzer, and C.-O. Olsson, "HVDC cable systems—Highlighting extruded technology," *IEEE Trans. Power Del.*, vol. 29, no. 1, pp. 414–421, Feb. 2014.
[6] G. Chen and A. E. Davies, "The influence of defects on the short-term breakdown characteristics and long-term DC performance of LDPE insulation," *IEEE Trans. Dielectr. Electr. Insul.*, vol. 7, no. 3, pp. 401–407, Jun. 2000.
[7] G. C. Montanari, C. Laurent, A. Campus, U. H. Nilsson, and G. Teyssedre, "From LDPE to XLPE: Investigating the change of electrical properties. Part I. Space charge, conduction and lifetime," *IEEE Trans. Dielectr. Electr. Insul.*, vol. 12, no. 3, pp. 438–446, Jun. 2005.
[8] H. R. Zeller and W. R. Schneider, "Electrofracture mechanics of dielectric aging," *Appl. Phys.*, vol. 56, no. 2, pp. 455–459, Feb. 1984.
[9] L. Dissado, G. Mazzanti, and G. C. Montanari, "The incorporation of space charge degradation in the life model for electrical insulating materials," *IEEE Trans. Dielectr. Electr. Insul.*, vol. 2, no. 6, pp. 1147–1158, Jan. 1996.
[10] T. Baumann, B. Fruth, F. Stucki, and H. R. Zeller, "Field-enhancing defects in polymeric insulators causing dielectric aging," *IEEE Trans. Electr. Insul.*, vol. 24, no. 6, pp. 1071–1076, Dec. 1989.
[11] S. Magdo, "Theory and operation of space-charge-limited transistors with transverse injection," *IBM J. Res. Develop.*, vol. 17, no. 5, pp. 443–458, Sep. 1973.
[12] G. C. Montanari, "Electrical life threshold models for solid insulating materials subjected to electrical and multiple stresses. I. Investigation and comparison of life models," *IEEE Trans. Electr. Insul.*, vol. 27, no. 5, pp. 974–986, Oct. 1992.
[13] *Standard Test Method for Dielectric Breakdown Voltage and Dielectric Strength of Solid Electrical Insulating Materials at Commercial Power Frequencies*. Standard ASTM D149-2009, 2013.
[14] J. H. Mason, "Effects of thickness and area on the electric strength of polymers," *IEEE Trans. Electr. Insul.*, vol. 26, no. 2, pp. 318–322, Apr. 1991.
[15] K. Kato, X. Han, and H. Okubo, "Insulation optimization by electrode contour modification based on breakdown area/volume effects," *IEEE Trans. Dielectr. Electr. Insul.*, vol. 8, no. 2, pp. 162–167, Apr. 2001.
[16] L. Zhao, J. Su, Y. Pan, R. Li, B. Zeng, J. Cheng, and B. Yu "Correlation between volume effect and lifetime effect of solid dielectrics on nanosecond time scale," *IEEE Trans. Dielectr. Electr. Insul.*, vol. 22, no. 4, pp. 1769–1776, Aug. 2015.
[17] U. Riechert, M. Eberhardt, J. Speck, and J. Kindersberger, "Breakdown behaviour of polyethylene at DC voltage stress," in *Proc. IEEE 6th Int. Conf. Conduction Breakdown Solid Dielectr. (ICSD)*, Jun. 1998, pp. 510–513.

[18] R. Khazaka, M. Bechara, M.-L. Locatelli, and S. Diaham, "Parameters affecting the DC breakdown strength of parylene F thin films," in *Proc. Annu. Rep. Conf. Electr. Insul. Dielectr. Phenom. (CEIDP)*, Oct. 2011, pp. 740–743.
[19] L. Z. Wang, "Effect of voltage waveform and thickness of sample on breakdown voltage strength," *Telecommun. Eng.*, no. 4, pp. 98–101, 1981.
[20] X. Li, J. Li, J. Zhang, L. Bao, H. Ran, and C. Xiang, "The influence of oil-impregnated insulation paper's thickness on electrical breakdown strength," in *Proc. IEEE Annu. Rep. Conf. Electr. Insul. Dielectr. Phenom. (CEIDP)*, Oct. 2016, pp. 392–395.
[21] S. Konzelmann and D. Peier, "Electric strength and dieletric properties of μm -polymer-films," in *Proc. IEEE Inter. Conf. Solid Dielectr. (ICSD)*, Jul. 2010, pp. 1–4.
[22] *Standard Pulsed Electro-Acoustic Test Method for Space Charge Measurement in Solid Insulating Materials*. Standard JB/T 12927-2016, 2016.
[23] G. C. Montanari and D. Fabiani, "Evaluation of DC insulation performance based on space-charge measurements and accelerated life tests," *IEEE Trans. Dielectrics Electr. Insul.*, vol. 7, no. 3, pp. 322–328, Jun. 2000.
[24] L. A. Dissado, C. Laurent, G. C. Montanari, and P. H. F. Morshuis, "Demonstrating a threshold for trapped space charge accumulation in solid dielectrics under DC field," *IEEE Trans. Dielectrics Electr. Insul.*, vol. 12, no. 3, pp. 612–620, Jun. 2005.
[25] A. John, *Extruded Cables for High-Voltage Direct-Current Transmission*. Piscataway, NJ, USA: IEEE Press, 2013, pp. 112–122.
[26] H.-R. Bian, L.-J. Yang, Z.-P. Ma, Z.-X. Li, X.-E. Wang, Y. Yuan, and R.-Y. Yao, "Method of selecting step stress test parameters for XLPE insulation DC voltage endurance coefficient," *IEEE Trans. Dielectr. Electr. Insul.*, vol. 26, no. 3, pp. 746–753, Jun. 2019.
[27] X. Wang, C. Chen, K. Wu, M. Fu, S. Hou, and J. Xiong, "PEA space charge measurement technology for full-scale cables based on pulse injection from outer semi-conductive layer," *High Voltage Eng.*, vol. 43, no. 5, pp. 1677–1683, May 2017.
[28] S. Hou, M. L. Fu, and Y. Tian, "PEA method based full-size DC cable space charge measurement system design and acoustic signal attenuation and dispersion correction," *Southern Power Syst. Technol.*, vol. 9, no. 10, pp. 37–41, 2015.

ZHIPENG MA was born in China, in 1988. He is currently pursuing the Ph.D. degree with the College of Electrical Engineering, Chongqing University, China. His major research interests include influence of space charge on insulation characteristics of cable breakdown and dielectric behavior of insulation material.

LIJUN YANG was born in China, in 1980. She received the M.S. and Ph.D. degrees in electrical engineering from Chongqing University, China, where she is currently pursuing a Professor with the Electrical Engineering College. Her research interests include on-line monitoring of insulation condition and fault diagnosis for high voltage apparatus, as well as aging mechanism and diagnosis for power transformer.

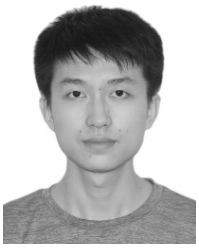

HAORAN BIAN was born in China, in 1994. He is currently pursuing the Ph.D. degree with the College of Electrical Engineering, Chongqing University, China. His major research interests include the field of aging mechanism and space charge effect for power cable.

MUHAMMAD SHOAIB BHUTTA was born in Pakistan, in April 1988. He received the M.Sc. degree in electrical engineering from Chongqing University, Chongqing, China, in 2014, where he is currently pursuing the Ph.D. degree in electrical engineering. His research interests include high voltage and its insulation includes HVDC insulation, nano dielectric, and breakdown testing.

PENGFEI XU was born in China, in 1995. He is a currently pursuing the M.Sc. degree with the College of Electrical Engineering, Chongqing University, China. His major research interest includes influence of space charge on insulation characteristics of cable.